

METAMAGNETISM IN MnMg FERRITE: MEDIUM FOR MAGNETIC CLOAK AND SHIELDING

Jozef Sláma* – Martin Šoka* – Vladimír Jančárik*

The metamagnetic transition (MT) from anti-ferromagnetic (AFM) to ferrimagnetic (FM) state by applying a magnetic field was studied in the Fe-deficient MgMn ferrite. It is presented that MgMn ferrite shows MT at temperature variations under applied field below the critical value of field strength H_t . The critical transition field $H_t = 580$ A/m was estimated for MT from the AFM to FM state from temperature dependence of remanent magnetic flux density. It is assumed, that the MT can be induced by changes of the anisotropy. In the studied magnetic system, the AFM state changes to FM state under the influence of magnetic field at adequate transition temperature T_t . One class of the MgMn ferrites that can become attractive are the metamagnetic systems. On base of studied ferrite can be constructed a cloak that can shield an object from a dc and/or ac magnetic field.

Keywords: metamagnetism, MnMg ferrite, magnetic cloak

1 INTRODUCTION

The magnetic properties of the MnMg ferrites are a matter of interest for next reasons. First, their study helps to interpret some of the fundamental principles of magnetism (magnetic order, Y-K canting interaction, crystal field effects, valence instabilities, magnetoelastic properties, coexistence of rectangular hysteresis loop). Second, they are of several application interest. They have interesting structural and magnetic properties and they can be used in many important components such as microwave devices, memory cores, transformers, chokecoils, highfrequency instruments and noise filters, owing to their high magnetic permeabilities and low magnetic losses. These properties are dependent on the nature of ions and their charge distribution among tetrahedral and octahedral sites. More recently, it was found that the metamagnetics exhibit magnetic properties of soft magnetic materials, analogously to further class of materials, and have attained considerable importance with regard to industrial application [1]-[4].

The metamagnetics can show antiferromagnetic response in different direction of magnetization. In a metamagnetic system, the AFM state changes to ferrimagnetic/ferromagnetic FM under the influence of magnetic field [4]. However, magnetic instability can be initiated with temperature due to a change in internal molecular field that affects the magnetic d-electron subsystems. Below its magnetic ordering temperature, a typical metamagnet is an antiferromagnet, but increasing the applied field strength can ultimately overcome the crystal anisotropy forces to change abruptly the internal magnetic structure. The resulting field-induced magnetic transition from a state of low magnetization to one of relatively high magnetization but with a low susceptibility in each case is called metamagnetism [5], [6]. The metamagnetic transitions from AFM to the FM state by

applying the magnetic field was discovered in the Fe-deficient MgMn ferrite and early published in [7-9]. In the present paper, we discuss the selected results of the investigation of metamagnetic effects of $\text{Mn}_{0.89}\text{Mg}_{0.3474}\text{Fe}_{1.758}\text{O}_{3.88}$ ferrite with rectangular hysteresis loop under influence of magnetic field and various temperatures. One important class of MnMg ferrites, due to their change of ground-states under magnetization, can become very attractive in the metamagnetic systems, and some of them could be an important step toward making a magnetic cloak.

2 EXPERIMENTAL

Non-stoichiometric MnMg ferrites were fabricated by a conventional ceramic processing method. The mixtures of Fe_2O_3 , MnO and MgO, were sintered at 1200°C . Studied $\text{Mg}_{0.347}\text{Mn}_{0.894}\text{Fe}_{1.758}\text{O}_{3.88}$ ferrite samples have rectangular hysteresis loop characterized by flat tops and relatively low coercivity. Samples were of toroidal shape with inner and outer diameters 3.9 mm and within interval $\langle 6.15 - 6.10 \rangle$ mm, respectively, so the measured samples did not been thin walled toroids here. The magnetization curves were measured by a conventional experimental set-up. Magnetic properties at low frequencies were evaluated from the set of minor loops measured by means of computer-controlled hysteresis graph built-up from commercially available measuring instruments. The experimental set-up allows usage of analogue (hardware) as well as digital (software) feedback to control the waveform shape of either exciting field $H(t)$ or flux density $B(t)$. The squareness of the hysteresis loop was characterized mainly by B_0 values of induction. The B_0 values were measured, when the core is in $+B_r$ state and subjected to an applied magnetic field $-H_a/2$ which will cause the hysteresis loop to be transversed to the induction $B_0 = B(-H_a/2)$ [10]. The H_a is amplitude of applied magnetic field.

* Institute of Electrical Engineering, Faculty of Electrical Engineering and Information Technology, Slovak University of Technology in Bratislava, Ilkovičova 3, 812 19 Bratislava, Slovakia; jozef.slama@stuba.sk

3 RESULTS AND DISCUSSION

Dependence of magnetic flux density amplitude B_a on magnetic field amplitude H_a at frequency $f = 50\text{Hz}$ at various temperatures was measured. Sample was heated from the room temperature up to Curie point $T_C = 297^\circ\text{C}$, then cooled down to -193°C (Fig. 1.). By cooling the sample, $B_a(T)$ curve at field $H_a = 580\text{ A/m}$ increases down to -193°C , see Fig. 1.

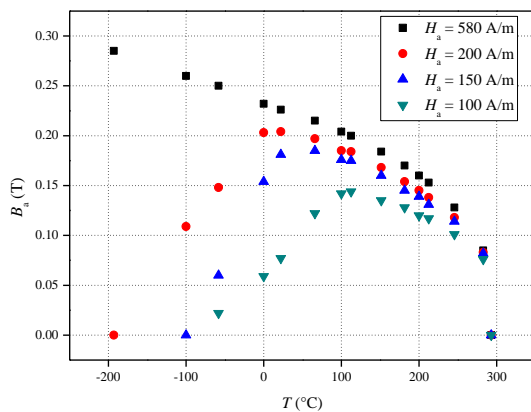


Fig. 1. The amplitude magnetic flux density B_a as functions of temperature T for applied fields $H_a = 580, 200, 150$ and 100 A/m

Changes of the temperature dependence of flux density at lower amplitudes of applied magnetic field $H_a = 200, 150$ and 100 A/m exhibit different behavior. Below the $H_a = 580\text{ A/m}$, the evolution of the flux density B_a as function of T is quite sensitive to field strength as well as the temperature at which the field is applied. As an example, by cooling the sample from T_C , the B_a at lower applied fields $H_a = 200\text{ A/m}$ increases up to 20°C and then flux density decreases significantly down to -200°C , where the curve reaches out zero value. In the ferrite, sharp magnetization step appears at low temperature. There is a field dependent transition temperature (-200°C) between the two magnetic phases. The transition is included in the category of metamagnetic transitions. $B_a(T)$ curve at applied field $H_a = 150\text{ A/m}$ increases from T_C up to 51.4°C ($B_a = 0.186\text{ T}$), and then decreases significant down to -100°C and the zero value reaches out. It is the other metamagnetic transition from between two magnetic states at $H_a = 150\text{ A/m}$. On other hand, the temperature dependence of B_a at more lower applied field $H_a = 100\text{ A/m}$ increases by cooling the sample from T_C up to 112°C and then B_a decreases significantly down to zero value at -85°C . It is again the other transition point at $H_a = 100\text{ A/m}$. From that the point of view, the $B_a(T)$ dependence measured at highest constant field 580 A/m present metamagnetic transition curve.

In following experiment using the same samples, remanent induction B_r upon cooling in a field of $H_a = 580, 200, 150$ and 100 A/m from T_C down to -193°C were measured. The data had different values with comparison to measured $B_a(T)$ curves depicted in Fig. 1. In the cooling

process at high field 580 A/m , the measured B_r temperature dependence have similar nature as $B_a(T)$ in Fig. 1. The remanent induction increases upon cooling the sample to $B_r = 0.257\text{ T}$ at -193°C and it is continuously increasing slightly up to lowest temperature. Below this transition field (580 A/m), the evolution of the B_r as function of temperature T is again sensitive to field strength and to the temperature at which the field is applied. Temperature dependence of B_r at lower applied fields $H_a < 580\text{ A/m}$ have similar nature as $B_a(T)$ curves depicted in Fig. 1. As the example, by cooling the sample from T_C , the $B_r(T)$ curve at applied field $H_a = 150\text{ A/m}$ increases up to 45°C and then induction decreases significant down to -100°C , which is illustrated in Fig 2.

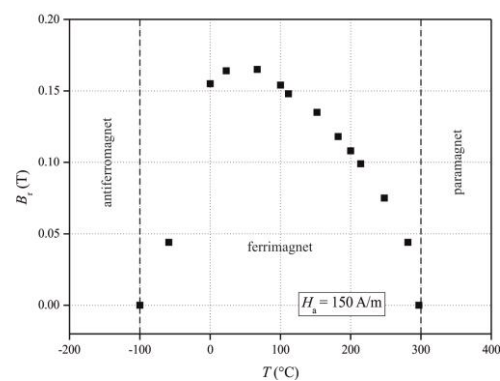
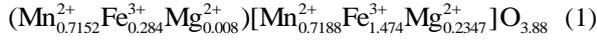


Fig. 2. Phase diagram of $\text{Mn}_{0.89}\text{Mg}_{0.3474}\text{Fe}_{1.758}\text{O}_{3.88}$ ferrite showing the three principal ground states for magnetization process at applied field $H_a = 150\text{ A/m}$

The curve can serve as an example of a magnetic phase diagram. The magnetic field temperature phase diagram shows different basic states of $\text{Mg}_{0.347}\text{Mn}_{0.894}\text{Fe}_{1.758}\text{O}_{3.88}$ selected for applied $H_a = 150\text{ A/m}$. The diagram is found to be composed of (at least) three different magnetic basic states. Below 0°C , the remanent induction decreases significantly down to -100°C and tending to zero value. Please note that magnetic state below -100°C up to -273°C is canted-antiferromagnetism measured in $H_a = 150\text{ A/m}$. The data above -100°C up to $T_C = 297^\circ\text{C}$ correspond to ferrimagnetic ground state in $H_a = 150\text{ A/m}$. At constant magnetic field (150 A/m), there is a continuous metamagnetic jump from a zero induction to a high one with the temperature T increasing in interval $-100^\circ\text{C} \leq T < 45^\circ\text{C}$. The data above -100°C up to 45°C are consistent probable with a canted-ferrimagnetic state at these temperatures in contrast to colinear-ferrimagnetic state in interval from 45°C up to $T_C = 297^\circ\text{C}$. The transition is from a canted-ferrimagnet to a ferrimagnet in maximum value of B_r at 45°C . The third basic phase above T_C is paramagnetic. Described phase diagram cannot be explained by Neel's model, but it can only be explained by a Yafet-Kittel (Y-K) canting. Such a result could be discussed assuming the following cation distribution: whilst 0.008 of Mg^{2+} , 0.284 Fe^{3+} and 0.7152 Mn^{2+} ions occupy the A site, the 0.1788 of Mn^{2+} , 1.474 Fe^{3+} and

0.2347 Mg^{2+} ions occupy the B site in spinel lattice. It reaches a theoretical value of magnetic moment according to the model



Such a cation distribution is based on the fact, that 80% of Mn^{2+} ions occupy the A-site while 20% occupy the B-site [11]. Thus, considering [12]-[15], the probable cation distribution of the parent MnMg ferrite is suggested as described by (1). Thus the theoretical total magnetic moment m_T can be estimated by an expression

$$\begin{aligned} & (5 \times 0.7152 + 5 \times 0.284 + 0 \times 0.008) \\ & \times [5 \times 0.1788 + 5 \times 1.474 + 0 \times 0.2347] \mu_B \\ & = (-4.996 + 8.264) \mu_B \end{aligned} \quad (2)$$

where the magnetic moment of Fe^{3+} and Mn^{2+} ions is $5 \mu_B$ (Bohr magneton) and of Mg^{2+} ions is $0.0 \mu_B$ per unit chemical formula. The () parentheses in the relation (1) denote the placement of the ions in A sites, meanwhile square brackets [] show the placement of the ions in B sites. The B sublattice is canted due to magnetostatic energy reduction. Thus the shape of phase diagram can only be explained by Y–K triangular magnetic ordering on B site ions leading to the change in A–O–B superexchange interactions due to changing temperature of sample at applied fields $H_a \leq 150$ A/m. Effective magnetic moments of A and B sublattices below the transition temperature $T_{t1} = -100^\circ\text{C}$ are mutually compensated. Therefore, the net magnetic moment is given by the vector sum of the moments of the two sublattices, *ie* $m_T = 0$. Thus the magnetic state below -100°C down to -273°C is canted-antiferromagnetism. This metamagnet displays a zero induction response in the applied fields $H_a \leq 150$ A/m, it means practical demon-

stration of a magnetic version of an “invisible” cloak. The m_T of both sublattices is positive,

$$m_T = m_B - m_A \geq 0 \quad (3)$$

above the transition temperature $T_{t1} = -100^\circ\text{C}$ up to transition point $T_{t2} = 45^\circ\text{C}$. It is consistent probable with a canted-ferrimagnetic ordering. Then m_T at the temperature $T = 45^\circ\text{C}$ up to $T_C = 297^\circ\text{C}$ is also positive, $m_T \geq 0$, but it is consistent with the collinear-ferrimagnetic state. The net magnetic moment at $T \geq T_C = 297^\circ\text{C}$ is zero.

Hysteresis loops were measured at the amplitude of field intensity 330 A/m at various temperatures (Fig. 3.). Note an unexpectedly highest loop (B_a value) at 0°C , in spite of that widest loop (highest coercive field) is at -193 A/m, although the height of this loop tends to be lower with decreasing temperature. Below -193°C , the height of the loop will be zero approximately at -253°C and the loop decays. On the other side, from 0°C up to T_C the B_a and coercive field decrease with temperature. The loop decays again at $T_C = 297^\circ\text{C}$.

A ferrite that exhibits rectangular hysteresis loop is capable of performing storage function as memory elements in computer systems, as logic and switching elements. When the core is in the $+B_r$ state and it is subjected to the applied field $-H_a/2$, the hysteresis loop is traversed to the induction B_0 , *ie* induction will fall to $B_0 = B(-H_a/2)$. Upon removing the field, the induction will rise slightly, following the minor loop, to B_r' , which is only slightly lower than $+B_r$. Subsequent applications and releases of the field $-H_a/2$ will result in the excursion of B around the minor loop between B_0 and B_r' .

Dependence of B_0 on magnetic field with amplitude H_a at temperatures $T = -59^\circ, 0^\circ, 22^\circ$ and 66°C is illustrated in Fig. 4.

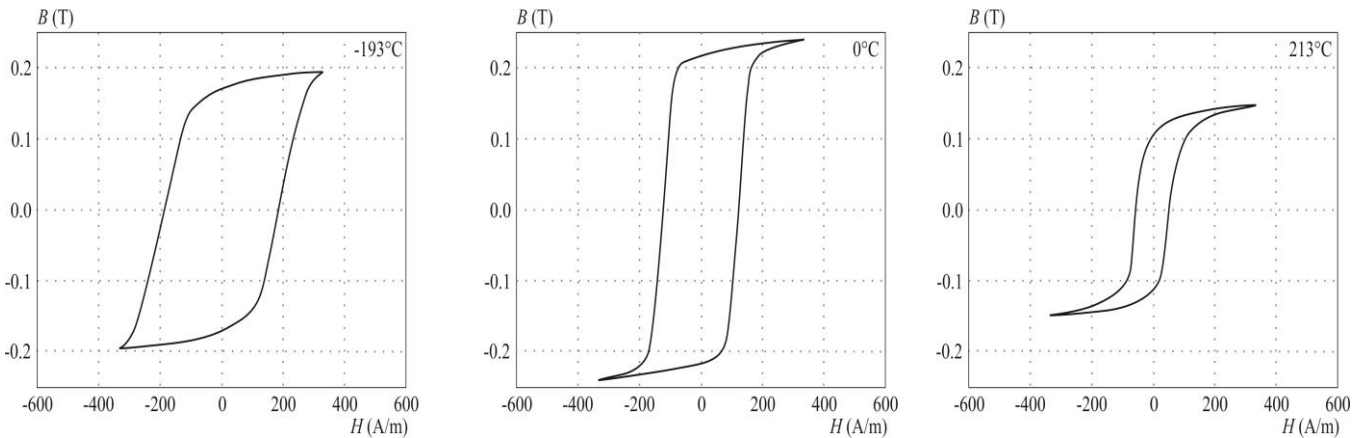


Fig. 3. Hysteresis loops measured at applied field $H_a = 330$ A/m for selected temperatures

The values of the $B_0(H_a)$ curves can be used to characterize the loop shape by the squareness ratio B_0/B_r at selected temperatures as well as a characterization curves of sensor medium to temperature stabilization,

detection or measurement of temperature by means of magnetic field. On the other hand, an artificial structure assembled from microscale components can be designed and fabricated. Structure consisting of array of selected

MnMg ferrites plates, can exhibit a highly anisotropic antiferromagnetic response (with B_r , $B_a = 0$) in defined dc and/or ac magnetic field at regarded temperature range (see Figs. 1, 2).

We believe that this is an important step toward making a magnetic cloak, a device that could guide magnetic fields around a shielded inner region while the leaving the outside field undisturbed.

The MnMg ferrite plates provide a base against the screening. Plates can be fabricated in squared lattice on flexible plastic substrates and a number of these layers can be stacked on top of each other. An applied field to thin plates can be barely identify around the plates. As one of example, the plates in antiferromagnetic state under magnetic fields $H_a \leq 150$ A/m provide a base for the screening, because magnetic moment of this MnMg ferrite is zero below -100°C . Using such ferrite a cloak can be designed that can shield an object from a dc and/or ac magnetic field. Demonstrating the anisotropic, tunable antiferromagnetic, it is a key step towards to construction of a magnetic version of an “invisibility” cloak at defined magnetic field and temperature range

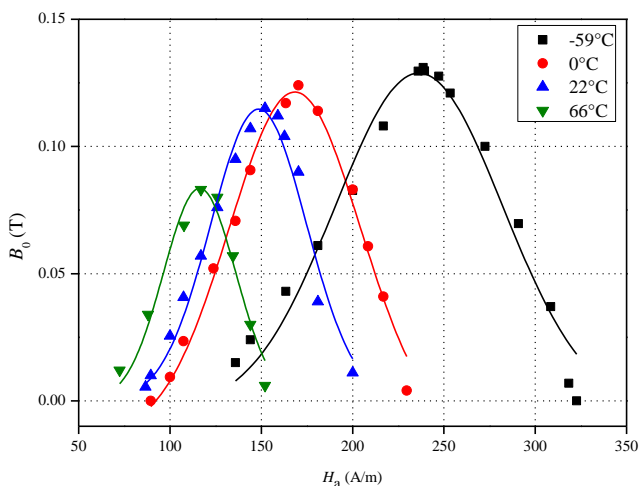


Fig. 4. The induction B_0 as functions of applied field H_a at various temperatures

4 CONCLUSION

This paper presents a brief review of existing work and original results on the metamagnetic behavior of substituted $\text{Mg}_{0.347}\text{Mn}_{0.894}\text{Fe}_{1.758}\text{O}_{3.88}$ ferrite. Below T_C , the temperature dependence of the flux density B_a and remanent flux density B_r is quite sensitive to field strength as well as the temperature at which the field is applied on the sample. It is possible to determine some specific features of the metamagnetic phenomenon and to formulate criteria to reveal such transitions in other spinel ferrites as well. We suggest that these observations are intrinsic to the chemical and structural nature of this compound. An example of MgMn ferrites that exhibits a sudden transition from the antiferromagnetic state to

a highly magnetized ferrimagnetic state under influence of magnetic field is the compound $\text{Mg}_{0.347}\text{Mn}_{0.894}\text{Fe}_{1.758}\text{O}_{3.88}$, which can be used in a process of target utilizing of ferrites for recording, pulse and digital applications, and a magnetic version of an invisibility cloak. The research on metamagnetics continues to attract the attention of wide-ranging scientific and engineering communities.

Acknowledgement

This work was supported by the Slovak Research and Development Agency under the contract No APVV -0062-11 and by the Scientific Grant Agency of the Ministry of Education, Science, Research and Sport of the Slovak Republic, and in part by the Slovak Academy of Sciences, under project No VG-1/0571/15 and project No 1/1163/12.

REFERENCES

- [1] ELOVAARA, T. – HUHTINEN, H. – MAJUMDAR, S. – PATURI, P.: Irreversible metamagnetic transition and magnetic memory in small-bandwidth manganite $\text{Pr}_{1-x}\text{Ca}_x\text{MnO}_3$ ($x = 0.0\text{--}0.50$), *J. Phys.: Condens. Matter* **24** No. 21 (2012), 216002.
- [2] KOLAT, V.S. – IZGI, T. – KAYA, A.O. – BAYRI, N. – GENCER, H., ATALAY, S.: Metamagnetic transition and magnetocaloric effect in charge-ordered $\text{Pr}_{0.68}\text{Ca}_{0.32-x}\text{Sr}_x\text{MnO}_3$ ($x = 0, 0.1, 0.18, 0.26$ and 0.32) compounds, *J. Magn. Magn. Mater.* **322** No. 4 (2010), 427-433.
- [3] TANG, T. – HUANG, R.S. – ZHANG, S.Y.: Ultra-sharp metamagnetic transition in manganite $\text{Pr}_{0.6}\text{Na}_{0.4}\text{MnO}_3$, *J. Magn. Magn. Mater.* **321** No. 4 (2009), 263–266.
- [4] KURMOO, M. – REHSRINGER, J.L. – HUTLOVA, A. – D’ORLÉANS, C. – VILMINOT, S. – ESTOURNÉS, C. – NIZNANSKY, D. *American Chemical Society* **17**(2005), 1106.
- [5] Hurd, C. M. *Contemporary Physics* **23** (1982), 469.
- [6] STRYJEWSKI, E. – GIORDANO, N. *Advances in Physics* **26** (1977), 487.
- [7] SLÁMA, J.: Experimental investigation the temperature dependences of static and dynamic properties of ferrites with SHL, Diploma Thesis SVŠT Bratislava (1962).
- [8] BENDA, O. – HORVÁTH, P. – SLÁMA, J. – VIRSÍK, F.: Experimental investigation the magnetic properties of ferrites with square hysteresis loop, *Proceeding EF SVŠT* (1963), 123.
- [9] BENDA, O. – HORVÁTH, P. – SLÁMA, J. – VIRSÍK, F. *Slaboproudý obzor* **26** (1965), 113.
- [10] CHEN, CH.-W.: *Magnetism and Metallurgy of Soft Magnetic Materials*, North-Holland Publishing Company (1977), 411-414
- [11] PATIL, F. – LENGLET M.: Spectroscopic evidence of the $\text{Mn}^{3+}\text{--}\text{Fe}^{2+}$ octahedral pair in lithium-manganese ferrites near the order-disorder transition. *Solid State Commun.* **86** No. 2 (1993), 67–71.
- [12] HEMEDA, O.M. *J. Magn. Magn. Mater.* **364** (2014), 39–46.
- [13] ELTABEY, M.M. – AGAMI, W.R. – MOHSEN, H.T.: Improvement of the magnetic properties for Mn–Ni–Zn ferrites by rare earth Nd^{3+} ion substitution, *J. Adv. Res.* **5** (2014), 601–605.
- [14] MANSOUR, S.F.: Structural and magnetic investigations of sub-nano Mn–Mg ferrite prepared by wet method, *J. Magn. Magn. Mater.* **323** No. 13 (2011) 1735–1740.
- [15] SINGH, M.: A comparative study of the electrical and the magnetic properties and Mössbauer studies of normal and hot pressed $\text{Mg}_x\text{Mn}_{1-x}\text{Fe}_2\text{O}_4$ ferrites, *J. Magn. Magn. Mater.* **299** No. 2 (2006), 397-403.

